Conference paper
UDC 535.37, 535.33
DOI: https://doi.org/10.18721/JPM.191.116

Room temperature microlasers based on quasi-planar geometry

A.V. Babichev [1]✉, Ya.N. Kovach [1], A.S. Dragunova [2], I.S. Makhov [2], N.V. Kryzhanovskaya [2], Yu.M. Zadiranov [1], Yu.A. Salii [1], M.M. Kulagina [1], M.A. Bobrov [1], A.P. Vasiliev [1], S.A. Blokhin [1], N.A. Maleev [2], L.Ya. Karachinsky [3], I.I. Novikov [3], A.Yu. Egorov [3]

[1] Ioffe Institute, St. Petersburg, Russia;
[2] National Research University Higher School of Economics, St. Petersburg branch, St. Petersburg, Russia;
[3] ITMO University, St. Petersburg, Russia
✉ a.babichev@mail.ioffe.ru

Abstract. The planar microcavity structure was grown using molecular-beam epitaxy. Single-mode lasing was observed at a wavelength of 960 nm for pillars with a diameter of 15 μm. At 300 K, the lasing threshold was approximately 30 mW. Increasing the pump power to 2.7 times the threshold power resulted in a mode energy shift of approximately 1 meV. This shift in the mode energy position corresponds to approximately 12 degrees of laser heating.

Keywords: molecular-beam epitaxy, micropillar cavity, gallium arsenide, InGaAs, Stransky-Krastanow growth mode

Funding: The work of A.V. Babichev, Ya.N. Kovach, A.S. Dragunova, A.P. Vasil'ev, and S.A. Blokhin was supported by the grant of the Russian Science Foundation (project no. 22-19-00221-П), https://rscf.ru/project/22-19-00221/ in the part of MBE epitaxy, and the study of photoluminescence spectra. The work of I.S. Makhov and N.V. Kryzhanovskaya was supported by the project of the Basic Research Program at the HSE University (project no. HSE-BR-2025-069) in the part of the analysis of the spectra of the test structure.

Citation: Babichev A.V., Kovach Ya.N., Dragunova A.S., Makhov I.S., Kryzhanovskaya N.V., Zadiranov Yu.M., Salii Yu.A., Kulagina M.M., Bobrov M.A., Vasil'ev A.P., Blokhin S.A., Maleev N.A., Karachinsky L.Ya., Novikov I.I., Egorov A.Yu., Room temperature microlasers based on quasi-planar geometry, St. Petersburg State Polytechnical University Journal. Physics and Mathematics. 19 (1.1) (2026) 98–104. DOI: https://doi.org/10.18721/JPM.191.116

Конференционная статья
УДК 535.37, 535.33
DOI: https://doi.org/10.18721/JPM.191.116

Микролазеры на основе квази-планарной геометрии, работающие при комнатной температуре

А.В. Бабичев [1]✉, Я.Н. Ковач [1], А.С. Драгунова [2], И.С. Махов [2], Н.В. Крыжановская [2], Ю.М. Задиранов [1], Ю.А. Салий [1], М.М. Кулагина [1], М.А. Бобров [1], А.П. Васильев [1], С.А. Блохин [1], Н.А. Малеев [1], Л.Я. Карачинский [3], И.И. Новиков [3], А.Ю. Егоров [3]

[1] Физико-технический институт им. А.Ф. Иоффе РАН, Санкт-Петербург, Россия;
[2] Национальный исследовательский университет "Высшая школа экономики", Санкт-Петербургский филиал, Санкт-Петербург, Россия;
[3] Университет ИТМО, Санкт-Петербург, Россия;
✉ a.babichev@mail.ioffe.ru

Аннотация. Гетероструктура планарного микрорезонатора была выращена методом молекулярно-пучковой эпитаксии. Продемонстрирована одномодовая генерация на длине волны 960 нм для микролазеров с диаметром 15 мкм. При температуре 300 K порог генерации составлял приблизительно 30 мВт. Превышение пороговой мощности в 2.7 раза привело к сдвигу положения энергии кванта, соответствующей длине волны генерации, около 1 мэВ. Данное смещение положения энергии кванта соответствует нагреву лазера около 12 градусов.

Ключевые слова: молекулярно-пучковая эпитаксия, микрорезонатор, арсенид галлия, InGaAs, режим роста Странского-Крастанова

Финансирование: Работа А.В. Бабичева, Я.Н. Ковача, А.С. Драгуновой, А.П. Васильева и С.А. Блохина выполнена при финансовой поддержке Российского научного фонда (проект № 22-19-00221-П), https://rscf.ru/project/22-19-00221/ в части эпитаксии методом молекулярно-пучковой эпитаксии и исследования спектров фотолюминесценции. Работа И.С. Махова и Н.В. Крыжановской выполнена при финансовой поддержке Программы фундаментальных исследований НИУ ВШЭ (проект № HSE-BR-2025-069) в части анализа спектров фотолюминесценции тестовых структур.

Ссылка при цитировании: Бабичев А.В., Ковач Я.Н., Драгунова А.С., Махов И.С., Крыжановская Н.В., Задиранов Ю.М., Салий Ю.А., Кулагина М.М., Бобров М.А., Васильев А.П., Блохин С.А., Малеев Н.А., Карачинский Л.Я., Новиков И.И., Егоров А.Ю. Микролазеры на основе квази-планарной геометрии, работающие при комнатной температуре // Научно-технические ведомости СПбГПУ. Физико-математические науки. 2026. Т. 19. № 1.1. С. 98–104. DOI: https://doi.org/10.18721/JPM.191.116

Introduction

Reservoir computing (RC) is one of the effective ways to implement neuromorphic computing due to its ability to efficiently learn through linear regression and classification. Compared with the electrical implementation of the RC, its optical implementation is promising due to its large scalability and large speed. In particular, RC based on diffractively coupled (DC) laser arrays made it possible to realize gigahertz speeds. In this case, the system bandwidth is determined by the internal dynamics of the lasers and the roundtrip time for light to pass through the external optics (~nanoseconds).

Current-injected vertical-cavity surface-emitting lasers (VCSELs) [1 – 4] and optically pumped micropillar cavity lasers [5 – 9] can serve as laser sources that provide DC. Both of these types of vertical microcavity lasers provide the vertical emission and array fabrication required for DC operation. The current-injected VCSEL array with a quantum wells (QWs) active region allows for diffractive coupling to be realized at room temperature [1], but the maximum element size in the array does not exceed 24 [1], which is due to the large pitch of the lasers on the substrate (≥80 μm [5]). In addition, the emission wavelength of individual current-injected VCSELs varies, and this can hardly be compensated due to wavelength tuning induced by the injection current [5]. Optically pumped microlasers with an active region based on quantum dots (QDs) provide a small element pitch (≤10 μm) and enable DC via injection locking, but do not provide lasing at room temperature. The emission wavelength of individual optically pumped microlasers can be precisely compensated by adjusting the pillar diameter [5]. As a result, it is possible to fabricate dense, spectrally homogeneous arrays of microlasers required for RC [5].

The low operating temperatures of optically pumped micropillar cavity lasers are due to optical absorption in mirrors at the pump wavelength and the low material gain of the active regions. The use of active regions based on QWs, whose gain is significantly larger than that of QDs, in the fabrication of microlasers is very limited. Due to the small diameter of the pillar cavity, large non-radiative surface recombination limits the possibility of continuous-wave (CW) operation of the QWs-based microlaser even at low-temperatures. In contrast, the tight confinement of charge

carriers in QDs reduces this effect. The use of mirrors based on GaAs/$Al_{0.9}Ga_{0.1}As$ layers, as well as an active region based on InGaAs QDs makes it possible to implement lasing action at 130 K for a microlaser with a diameter of 5 μm [10], which was the maximum operating temperature for micropillar lasers based on GaAs/$Al_{0.9}Ga_{0.1}As$ mirrors. In fact, strong optical absorption in the output mirror layers (GaAs) at the pump wavelength limits the power-conversion efficiency (PCE) to about 3%. Using resonant pumping of the wetting layer (WL) states (pumping in the range of 905–922 nm [10]) allows to mitigate the absorption in the output mirror layers. At the same time, due to the extremely small thickness of the WL, the absorption of the active region is negligible, resulting in a PCE value of less than one percent [10].

To implement laser operation at elevated temperatures, low absorbing (at the pump wavelength) mirrors based on $Al_{0.2}Ga_{0.8}As/Al_{0.9}Ga_{0.1}As$ layers were invented [11]. These low-absorption mirrors allow the PCE to be increased by approximately ten times (up to ~30% [11,12]). Increasing the number of QDs layers from one [11] to three allows for compensation of the increase in internal optical loss with increasing temperature. In this case, the maximum operating temperature does not exceed 220 K [6, 7]. For practical application of micropillar cavity lasers, it is necessary to ensure operation at room temperature.

This paper discusses the first results of studies of micropillar cavity lasers operating at room temperature, which was the main goal of the study.

Materials and Methods

The growth of a planar cavity structure was carried out using molecular-beam epitaxy (MBE). The optical length of the GaAs microcavity was one wavelength divided by the refractive index (1 λ microcavity). The microcavity was formed by distributed Bragg reflectors based on Al0.2Ga0.8As/$Al_{0.9}Ga_{0.1}As$ layers. Compared with previous microcavities based on $Al_{0.2}Ga_{0.8}As/Al_{0.9}Ga_{0.1}As$ mirrors (based on 35 and 27 pairs in the bottom and top mirrors [7]), the modelled quality factor (Q-factor) of the cold cavity (excluding the absorption of the active region) increased more than twofold. The number of pairs in the bottom and top mirrors was 35 and 31, respectively. Three layers of QDs were used as the active region. QDs were self-assembled from $In_{0.5}Ga_{0.5}As$ using Stranski-Krastanov growth method and located in the center of the cavity, at the optical field node. Compared to the previous [7], changing the growth conditions eliminates vertical alignment of QDs. This leads to an increase in the material gain of the active region [13]. To fabricate the micropillar cavities, a dry etching process was performed through a mask of reflowed photoresist.

For optical characterization, the samples were placed in an optical cryostat (Cryostation® s50, Montana Instruments). The temperature of samples during the study was fixed at 300 K. A semiconductor laser diode with a wavelength of 808 nm was used for optical pumping in CW mode. For optical pumping, a 20× objective (Mitutoyo M Plan Apo NIR) with a focal spot size of 4 μm was used. The reduction in the pumping spot size (pumping the central part of the pillar) compared to previous ones [6, 7, 11], allows for lateral heat extraction and minimizing heating of the active region. An SR-500i spectrograph (Andor Shamrock) was used to collect spectra at different pump powers. A diffraction grating with 1200 slits per millimeter limits the spectral resolution to 0.05 nm.

Results and Discussion

Single-mode emission was observed at a wavelength of 960 nm for a pillar with a diameter of 15 μm. To analyze the input-output (I-O) characteristic, the luminescence peak was fitted at different pump powers. The pseudo-Voigt function was used to determine the integrated intensity and linewidth in analogy with [11]. A superlinear (S-shaped) increase in the I-O characteristic (on a double logarithmic scale) was demonstrated, which, along with the narrowing of the luminescence peak (the Full Width at Half Maximum, FWHM, decreases from 0.2 to 0.05 nm, see Fig. 1, *a*), confirms the transition to lasing in microlaser with a diameter of 15 μm. To determine the lasing threshold and the Q-factor at threshold pump power, the I-O characteristic was fitted using an expression determined by solving the rate equations [10, 14]: $P_{pump}(P_{out}) = A\gamma/\beta[BP_{out}(1 + \xi)(1 + \beta BP_{out})/(1 + BP_{out}) - \beta\xi BP_{out}]$, where P_{pump} and P_{out} are the pump and output power, A and B are the input and output scaling factors, β is the fraction of the total spontaneous emission coupled to the lasing mode (spontaneous emission factor) [14]. The dimensionless factor ξ can be determined by: $\xi = n_0\beta/\gamma\tau_{sp}$, where n_0 is the exciton number at transparency threshold, τ_{sp} is the spontaneous

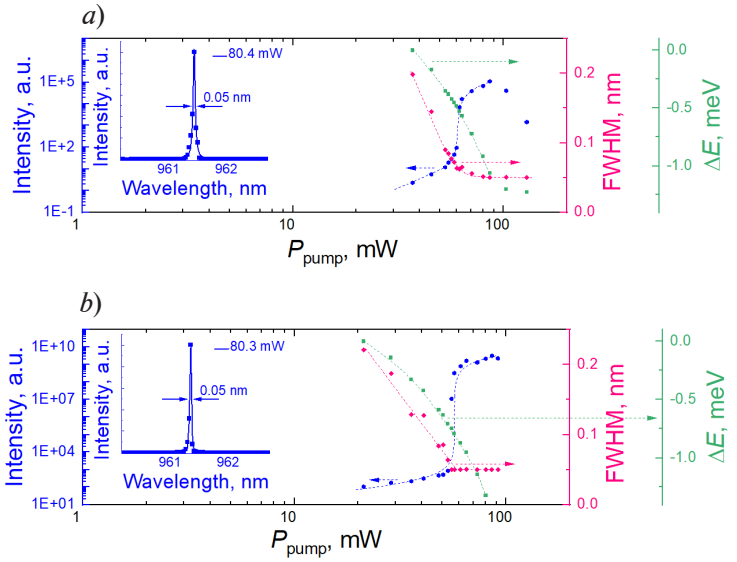

Fig. 1. Integrated intensity (left *Y*-axis), linewidth, and mode energy shift (right *Y*-axes) obtained at different pump powers. The dots on the panels correspond to experimental data, the dashed blue lines to intensities, the dashed red lines to linewidths, and dashed green lines to mode energy shifts. Panel (*b*) shows results for a pillar whose position on the substrate is shifted by 2760 μm compared to the pillar shown in panel (*a*).

The insets show the lasing spectrum at a pump power of 80.4 mW (panel *a*) and 80.3 mW (panel *b*)

emission lifetime, and γ is the cavity decay rate. To determine the value of γ, one can use the expression $\gamma = 2\pi v_L/Q$, where v_L is the lasing frequency and Q is the quality-factor determined at threshold pump power. To fit the *I-O* characteristic, $\tau_{sp} = 1$ ns can be used [10]. The value of n_0 can be determined from the QDs density and the effective size of the optical aperture as mentioned previously [5] and is equal to 22500. When fitting the *I-O* characteristics, β-factor was used as a fitting parameter and the value of ξ was fixed at 1.8. The latter was determined by specifying the values of γ, τ_{sp} and n_0. The best-fit value of the spontaneous emission factor in the laser mode is $7.5 \cdot 10^{-4}$%. The results of the fitting are shown in Fig. 1 (dotted *S*-shaped line on the left *Y* axis). Assuming that the mean photon number in the mode is unity at the threshold [14] ($BP_{out} = 1$), the lasing threshold P_{th} can be extracted from the reduced expression: $P_{th} = A\gamma/2\beta[\xi(1 - \beta) + 1 + \beta]$. Using this expression, the lasing threshold is determined, which is 32 mW. The *Q*-factor at threshold pump power is 4400. A further increase in the pump power leads to an increase in the *Q*-factor to at least 19300 (see Fig. 1, *a*, right *Y*-axis), which is limited by the spectral resolution of the monochromator used. It also should be noted that the deviation from *S*-type *I-O* characteristic is observed at pump power more than 86 mW, which may be caused by extreme heating of the sample. To assess this issue, mode energy shift (ΔE) analysis was previously used [6, 7, 11]. If there is no additional heating, at low pump power, band filling and the plasma effect cause a blue shift in the mode energy. A further increase in pump power leads to a blue shift caused by an increase in the free carrier density [11]. Conversely, if thermal heating is present, then with increasing pump power the thermal effect dominates over others, causing a red shift of the mode energy. A similar behavior of the mode energy as a function of the pump power (red shift) is demonstrated in the examined pillar (see Fig. 1, right *Y*-axis). Increasing the pump power from 37 to 86 mW results in a red shift of the mode energy above 1 meV. Based on the mode energy shift as a function of temperature (T) [7], a rough estimate of sample heating can be made. At low temperatures, the $\Delta E/\Delta T$ dependence is nonlinear; at elevated temperatures, it can be approximated by a linear fit with a slope of ~0.08 meV/K. Taking this value into account, the heating of the microcavity laser is approximately 12 degrees at a pump power of 86 mW.

To study the spectral homogeneity over the substrate surface, the output characteristics of a micropillar laser were investigated, the position of which on the substrate was shifted by 2760 μm compared to the position of the micropillar described above and shown in Fig. 1, *a*. The pillar diameter was similar to the previous one (15 μm). A clear *S*-shaped *I-O* characteristic (on a double logarithmic scale) was also demonstrated, which, together with the reduction of FWHM

from 0.22 to 0.05 nm (see Fig. 1, *b*), confirms the laser action. The lasing threshold extracted from the rate-equations analysis is 29 mW. The small difference between the lasing threshold and the similar value discussed above (32 mW) may be associated with a change in the magnitude of the gain to cavity detuning, which varies across the substrate due to variations in the thickness of the epitaxial layers across the substrate. A spectral nonuniformity of 29 meV along the radius of a 2-inch wafer was previously reported for a planar cavity structure grown by metal-organic vapor phase epitaxy (MOVPE) [5], which is associated with a thickness variation of approximately 2%. In contrast, for the planar microcavity grown by the MBE, the thickness change is less than one percentage, resulting in a resonance energy shift that is 7 times smaller [12] compared to its MOVPE-grown counterpart. As a result, this is the main reason for the low difference in the lasing threshold across the substrate surface. The lasing wavelength just above the threshold is 960.46 nm for the second micropillar, which differs from the similar value discussed above by approximately 0.21 nm (279 μeV). A resonance mode variation of approximately 1 meV along a 64×64 μm^2 array with a standard deviation of 342 μeV was previously reported [4]. As a result, a resonance difference of approximately 280 μeV, achieved in an experiment with a shift along the substrate of ~2.8 mm, demonstrates the potential for fabricating highly uniform arrays of QDs micropillars required for RC using the MBE growth method.

For comparative analysis with previous studies, it should be noted that the maximum operating temperature of lasers with low-absorption mirrors (based on $Al_{0.2}Ga_{0.8}As/Al_{0.9}Ga_{0.1}As$ layers) and microcavities grown by MBE and MOVPE is 220 [7] and 200 K [6]. Further increase in the operating temperature is limited by thermal heating of the sample, which occurs until the lasing threshold is reached. To address this issue, a pumping scheme with a point focus in the central region of the pillar was implemented, allowing for additional lateral heat dissipation, similar to VCSELs with a buried tunnel junction [2, 3]. Furthermore, the *Q*-factor of the vertical microcavity more than doubled, and the material gain increased due to the absence of vertical positioning of the vertically stacked QDs layers. As a result, optimization of the optical pumping method and design optimization will make it possible to operate microcavity lasers at room temperature.

Conclusion

Optically pumped microlasers operating at room temperature are needed for the development of quantum photonics, integrated photonic circuits [6] and reservoir computing [5]. This work demonstrates the possibility of operating micropillar cavity lasers at room temperature. At the same time, doubling the pump power above the lasing threshold results in sample heating by more than 10 degrees. Further research will focus on analyzing pulse characteristics to minimize sample heating.

Recently, a photonic-defect cavity was used to achieve operation at room temperature [6]. While the bottom mirror is semiconductor-based, the top mirror is entirely dielectric. The thermal conductivity (κ) of SiN_x (the high-refractive index material in the pair) is approximately 2.5 times lower than that of $Al_{0.2}Ga_{0.8}As$. Moreover, the κ value of SiO_x (the low-refractive index material in the pair) is approximately 58 times lower than that of $Al_{0.9}Ga_{0.1}As$. These facts limit the heat dissipation through a dielectric mirror compared to its semiconductor counterpart. To demonstrate the practical application potential of the photonic defect cavity, further analysis of the heating (mode energy shift) is necessary.

The concept of a photonic-defect cavity based on entirely semiconductor mirrors could become an alternative to micropillar cavities but involves a two-step epitaxy process. In fact, before epitaxy of the top mirror, it is necessary to develop epitaxial layers for overgrowing the etched mesa. Two-step epitaxy of semiconductor mirrors on GaAs substrates was previously achieved [15], demonstrating the potential of a photonic defect cavity based on semiconductor quasi-planar geometry.

REFERENCES

1. **Pflüger M., Brunner D., Heuser T., Lott J. A., Reitzenstein S., Fischer I.,** Experimental reservoir computing with diffractively coupled VCSELs, Optics Letters. 49 (9) (2024) 2285–2288.

2. **Babichev A.V., Kovach Y.N., Blokhin S.A., Karachinsky L.Y., Novikov I.I., Egorov A.Y., Tian S.-C., Bimberg D.,** Long-wavelength VCSELs with buried tunnel junction: design optimization, JPhys Photonics. 7 (3) (2025) 032001.

3. **Babichev A., Blokhin S., Gladyshev A., Karachinsky L., Novikov I., Blokhin A., Bobrov M., Kovach Y., Kuzmenkov A., Nevedomsky V., Maleev N., Kolodeznyi E., Voropaev K., Vasilyev A., Ustinov V., Egorov A., Han S., Tian S.-C., Bimberg D.,** Impact of device topology on the performance of high-speed 1550 nm wafer-fused VCSELs, Photonics. 10 (6) (2023) 660.

4. **Blokhin S.A., Bobrov M.A., Blokhin A.A., Kuzmenkov A.G., Maleev N.A., Ustinov V.M., Kolodeznyi E.S., Rochas S.S., Babichev A.V., Novikov I.I., Gladyshev A.G., Karachinsky L.Ya., Denisov D.V., Voropaev K.O., Ionov A.S., Egorov A.Yu.,** Analysis of the internal optical losses of the vertical-cavity surface-emitting laser of the spectral range of 1.55 μm formed by a plate sintering technique, Optics Spectroscopy. 127 (1) (2019) 140–144.

5. **Heuser T., Grose J., Holzinger S., Sommer M. M., Reitzenstein S.,** Development of highly homogenous quantum dot micropillar arrays for optical reservoir computing, IEEE Journal of Selected Topics in Quantum Electronics. 26 (1) (2020) 1–9.

6. **Gaur K., Tripathi S., Laudani F., Barua A., Limame I., Koulas-Simos A., Rodt S., Reitzenstein S.,** Photonic-defect cavities as next-generation room-temperature microlasers: a comparative study with micropillars, Laser & Photonics Reviews. 19 (18) (2025) e00533.

7. **Babichev A., Makhov I., Kryzhanovskaya N., Blokhin A., Zadiranov Y., Salii Y., Kulagina M., Bobrov M., Vasil'ev A., Blokhin S., Maleev N., Tchernycheva M., Karachinsky L., Novikov I., Egorov A.,** Lasing of quantum-dot micropillar lasers under elevated temperatures, IEEE Journal of Selected Topics in Quantum Electronics. 31 (5) (2025) 1–8.

8. **Limame I., Shih C.-W., Koulas-Simos A., Pietsch J., Roche L. J., Plattner M., Koltchanov A., Rodt S., Reitzenstein S.,** Diameter-dependent whispering gallery mode lasing effects in quantum dot micropillar cavities, Optics Express. 32 (18) (2024) 31819–31829.

9. **Babichev A., Makhov I., Kryzhanovskaya N., Troshkov S., Zadiranov Y., Salii Y., Kulagina M., Bobrov M., Vasil'ev A., Blokhin S., Maleev N., Karachinsky L., Novikov I., Egorov A.,** Low-threshold surface-emitting whispering-gallery mode microlasers, IEEE Journal of Selected Topics in Quantum Electronics. 31 (2) (2025) 1–8.

10. **Andreoli L., Porte X., Heuser T., Große J., Moeglen-Paget B., Furfaro L., Reitzenstein S., Brunner D.,** Optical pumping of quantum dot micropillar lasers, Optics Express. 29 (6) (2021) 9084–9097.

11. **Shih C.-W., Limame I., Krьger S., Palekar C.C., Koulas-Simos A., Brunner D., Reitzenstein S.,** Low-threshold lasing of optically pumped micropillar lasers with $Al_{0.2}Ga_{0.8}As/Al_{0.9}Ga_{0.1}As$ distributed Bragg reflectors, Applied Physics Letters. 122 (15) (2023) 151111.

12. **Babichev A.V., Nikitina E.V., Karachinsky L.Ya., Novikov I.I., Egorov A.Yu.,** Planar micropillar cavity structure with enhanced power-conversion efficiency. In: Proceedings of the 2024 International Conference on Electrical Engineering and Photonics (EExPolytech), Saint Petersburg, Russia, 17 – 18 October 2024; Proc. IEEE. 2024. 266–269.

13. **Bimberg D., Grundmann M., Ledentsov N.N.,** Quantum Dot Heterostructures, John Wiley & Sons, New Jersey, United States. (1999).

14. **Bjork G., Yamamoto Y.,** Analysis of semiconductor microcavity lasers using rate equations, IEEE Journal of Quantum Electronics. 27 (11) (1991) 2386–2396.

15. **Egorov A.Y., Karachinsky L.Y., Novikov I.I., Babichev A.V., Berezovskaya T.N., Nevedomskiy V.N.,** Metamorphic distributed Bragg reflectors for the 1440–1600 nm spectral range: Epitaxy, formation, and regrowth of mesa structures, Semiconductors. 49 (10) (2015) 1388–1392.

THE AUTHORS

BABICHEV Andrey V.
a.babichev@mail.ioffe.ru
ORCID: 0000-0002-3463-4744

KOVACH Yakov N.
yakovachyakov@gmail.com
ORCID: 0000-0003-4858-4968

DRAGUNOVA Anna S.
anndra@list.ru
ORCID: 0000-0002-0181-0262

MAKHOV Ivan S.
imahov@hse.ru
ORCID: 0000-0003-4527-1958

KRYZHANOVSKAYA Natalia V.
nataliakryzh@gmail.com
ORCID: 0000-0002-4945-9803

ZADIRANOV Yuriy M.
Zadiranov@mail.ioffe.ru

SALII Yulia A.
Guseva.Julia@mail.ioffe.ru

KULAGINA Marina M.
Marina.Kulagina@mail.ioffe.ru

BOBROV Mikhail A.
bobrov.mikh@gmail.com
ORCID: 0000-0001-7271-5644

VASIL'EV Alexey P.
Vasiljev@mail.ioffe.ru
ORCID: 0000-0002-2181-5300

BLOKHIN Sergey A.
blokh@mail.ioffe.ru
ORCID: 0000-0002-5962-5529

MALEEV Nikolay A.
maleev@beam.ioffe.ru
ORCID: 0000-0003-2500-1715

KARACHINSKY Leonid Ya.
leonid.karachinsky@connector-optics.com
ORCID: 0000-0002-5634-8183

NOVIKOV Innokenty I.
innokenty.novikov@itmo.ru
ORCID: 0000-0003-1983-0242

EGOROV Anton Yu.
anton.egorov@connector-optics.com
ORCID: 0000-0002-0789-4241

Received 28.11.2025. Approved after reviewing 19.02.2026. Accepted 20.02.2026.